2020 IEEE International Conference on Robotics and Automation (ICRA)
31 May - 31 August, 2020. Paris, France

Position-based Impedance Control of a 2-DOF Compliant Manipulator for a Facade Cleaning Operation*

Taegyun Kim+, Sungkeun Yoo+, Hwa Soo Kim, *Member, IEEE,* TaeWon Seo, *Member, IEEE*

Abstract— **This paper presents the design of a compliant manipulator using a series elastic actuator (SEA) and a mechanism for precisely measuring the force acting on the contact part of the manipulator without using a force sensor. It is important to maintain a constant contact force between the compliant manipulator and the wall in order to guarantee cleaning performance, and the ball screw mechanism is used to adapt to changes in the distance and the angle. Position-based impedance control is used to maintain a constant contact force when the manipulator interacts with the wall of the building, and the results confirm that the system stability is guaranteed when using SEA, regardless of the variation in the actual stiffness of the manipulator. The results of extensive experimentation using the test bench demonstrate the force tracking performance against various types of wall changes using the stiff wet-type cleaning manipulator. The results indicate that the stiffness of SEA affects the force tracking performance and system stability under the condition of the manipulator and environment interaction, and that the system stability and control performance can be improved by applying a robust force measurement mechanism to noise.**

I. INTRODUCTION

Over the last decade, as the number of high-rise buildings has increased, so has the demand for wall cleaning. Cleaning the exterior walls of buildings is a difficult and dangerous task, since the worker must work on a rope or gondola in high altitude. Since the height, shape, and curvature of each building are different, there is no one product that can fully automate the cleaning of exterior walls. As a result, all of the cleaning work depends on the manual work of an operator. Therefore, substantial cleaning robot research has been conducted to fully automate the cleaning of the outer wall by replacing the operator.

To date, existing building cleaning robots have ascended and descended by the gantry on the roof of a building, and it has proven difficult to apply them to existing buildings because they must consider the initial design of buildings. In addition, the exterior walls of high-rise buildings can have various shapes and obstacles, but conventional robots can only overcome obstacles of limited heights and shapes [1]-[4].

Sky Cleaners ascends a building using a crane on the roof of the building and can overcome obstacles up to 60 mm. However, it is not applicable to curved walls because it is attached to the wall by vacuum pads [1]. Similar to Sky Cleaners, TITO500 and SIRIUSc ascend and descend by the gantry fixed on the roof [2,3]. However, these can only be used to clean flat walls, and it is difficult to apply them to curved walls or walls with obstacles. The building façade maintenance robot (BFMR) is a built-in type robot that allows for building cleaning to be fully automated [4]. However, it is essential to apply the BFMR at the design stage of a building, making it difficult to use in existing buildings.

Therefore, a novel 2-DOF compliant manipulator that can be installed in the gondola of a high-rise building is proposed. This manipulator can be easily applied to an existing building because it can be installed through an interface unit customized to the existing gondola. The ball-screw mechanism allows for the height and the angle between the wall and the manipulator to be adjusted simultaneously [5]. Further, since the manipulator has a modular cleaning part, it can be changed to the brush type or the squeegee type according to the degree of contamination of the wall.

In exterior wall cleaning, it is essential to maintain a constant contact force to ensure a consistent cleaning performance. In order to maintain a constant contact force despite the nonlinearity of the manipulator, a position-based impedance controller has been proposed [6], and a controller has been developed to both compensate for the disturbance and maintain the contact force in the presence of periodic disturbances [7]. However, due to the characteristics of the impedance controller, a difference between the actual impedance and the desired impedance can affect the stability and performance of the system. For example, if the value of the desired mass is smaller than the actual mass, the system becomes unstable, because the power required by the actuator to achieve reduced mass is greater [8]. Similarly, if the magnitude of the desired stiffness is less than the actual stiffness, stability cannot be guaranteed when the robotic manipulator interacts with a passive environment [9]. Generally, the exterior wall of the building has a higher stiffness than the manipulator, so the stability is affected by the manipulator stiffness in the interaction situation.

By adding compliance to the actuator stage of the cleaning manipulator, which has a modular design, various cleaning methods can be applied regardless of the stiffness of the end

+These authors have equally contributed to this paper as a first author.

* This research was supported by the National Research Foundation of Korea(NRF) Grant funded by the Ministry of Science and ICT for First-Mover Program for Accelerating Disruptive Technology Development(Management: NRF-2018M3C1B9088328 (2018M3C1B9088331, 2018M3C1B9088332)).

* This work was supported by the National Research Foundation of Korea(NRF) grant funded by the Korea government(MSIT) (No. 2019R1G1A1100785).

Corresponding authors (Hwa Soo Kim and TaeWon Seo)

T. Kim is with Mechanical Engineering, Yeungnam University, Gyeongsan 38641, Republic of Korea (email: tgkim@yu.ac.kr).

S. Yoo is with Mechanical and Aerospace Engineering, Seoul National University, Seoul 08826, Republic of Korea (email: skyoo@rodel.snu.ac.kr).

H. S. Kim is with Department of Mechanical System Engineering, Kyonggi University, Suwon 16227, Gyeonggi-do, Republic of Korea (e-mail: hskim94@kgu.ac.kr).

T. Seo is with the School of Mechanical Engineering, Hanyang University, Seoul 04763, Republic of Korea. (phone: +82-2-2220-0428, e-mail: taewonseo@hanyang.ac.kr).

part. It also makes it possible to control the force without a force sensor by estimating the force at the end using the displacement of the series elastic actuator.

In many cases, using force sensor data during force control can lead to system instability due to the presence of signal noise [10]. In this case, adding a filter to the sensor data to attenuate the noise affects the control performance because of the time delay. Therefore, this manipulator uses the method of measuring force from the displacement of SEA to minimize noise during force sensing and improve system stability. For this purpose, an encoder was attached to measure the position of the manipulator, and the differential kinematics of the manipulator allow for the contact force to be measured with an error within ± 5 %.

The rest of this paper is organized as follows. In section II, a 2-DOF compliant manipulator is introduced, and its kinematics and differential kinematics are analyzed. Section III presents stability analysis when applying a position-based impedance controller to the manipulator, including a series elastic actuator. In Section IV, the force tracking ability of the manipulator using the series elastic actuator is examined through extensive experimentation. Finally, conclusions are presented in Section V.

II. 2-DOF Compliant Manipulator For Façade Cleaning

A. Structure of Manipulator

Fig. 1(a) shows the cleaning unit attached to the gondola of a high-rise building. This manipulator can be attached to existing buildings by using interface units that can be customized to gondolas of various shapes. Fig. 1 (b) shows a wet-type cleaning unit with a nozzle for spraying water and a brush and a squeegee for removing contaminants from the wall. A cleaning module is attached to the end of the 2-DOF compliant manipulator, and the modular structure allows for different cleaning methods to be used. A detailed schematic diagram of the compliant manipulator is shown in Fig. 2. By adjusting the position of the joint using the left and right ball screw mechanism, the distance and angle between the wall and the manipulator can be adjusted by 170 mm and 12 degrees, respectively. In addition, the series elastic actuator capable of compliant motion is realized by adding a spring between the ball screw block and the joint connected to the lower part. In order to estimate the posture of the end effector, a linear encoder and a rotary encoder are attached to the block of the central linear shaft, and these are used to estimate spring displacement.

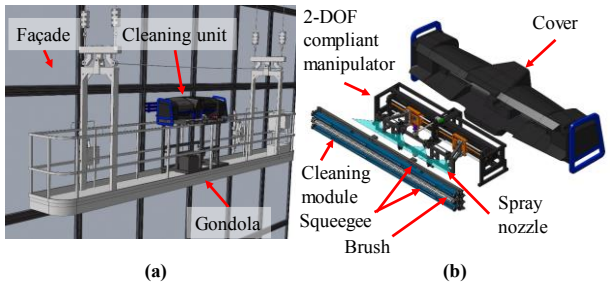

Figure 1. (a) Cleaning unit attached to the gondola (b) Schematic diagram of proposed cleaning unit

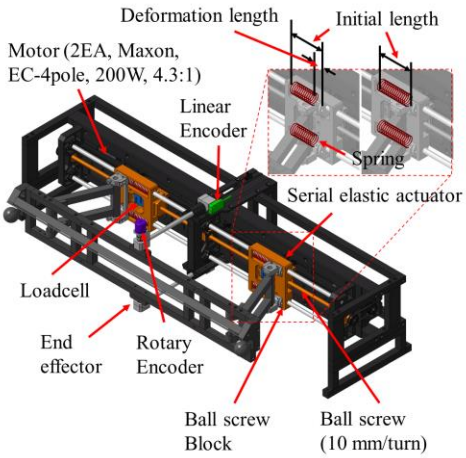

Figure 2. Schematic diagram of proposed 2-DOF compliant manipulator

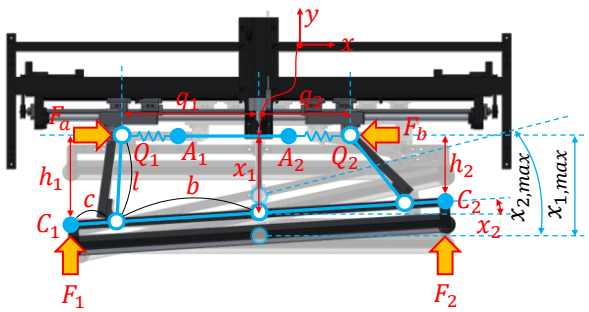

Figure 3. Kinematic model for proposed 2-DOF compliant manipulator

The cleaning unit cleans the exterior wall by using the brush and the squeegee of the manipulator to make contact with the wall, and cleaning proceeds when the applied contact force exceeds the specified force. However, the greater the contact force, the lower the stability of the manipulator's Gondola, so it is crucial to maintain a constant contact force to maintain a stable cleaning performance. Therefore, the force acting on the manipulator was measured by the spring displacement of the SEA, and a load cell was serially attached to the SEA to compare the measurement performance and the control performance.

B. Kinematic Analysis

Fig. 3 shows a kinematic model of the proposed 2-DOF compliant manipulator. The length of the contact point at the end of the manipulator can be obtained as follows from the linear encoder and the rotary encoder attached to the manipulator.

$$\begin{cases} h_1 = x_1 + (b+c)\sin x_2 \\ h_2 = x_1 - (b+c)\sin x_2 \end{cases}. \tag{1}$$

In order to obtain the displacement of the spring, it is necessary to know the location of the joints that are connected with a spring. Those also are calculated from encoders attached to the manipulator. The following constraint equation can be derived from the kinematic model.

$$\begin{cases} (q_1 - b\cos x_2)^2 + (x_1 + b\sin x_2)^2 = l^2 \\ (q_2 - b\cos x_2)^2 + (x_1 - b\sin x_2)^2 = l^2 \end{cases}. \tag{2}$$

Based on Eq. (2), the position of the joint is derived as follows.

$$\begin{cases} q_1 = b\cos x_2 - \sqrt{b^2\cos^2 x_2 - b^2 - x_1^2 - 2x_1 b\sin x_2 + l^2} \\ q_2 = b\cos x_2 - \sqrt{b^2\cos^2 x_2 - b^2 - x_1^2 + 2x_1 b\sin x_2 + l^2} \end{cases}. \quad (3)$$

The displacement of the spring is calculated according to the position of the ball screw block connected to the actuator. Therefore, the compressive force acting on the spring is obtained as

$$\begin{cases} F_a = k_s\left[d_i - \{q_1 - \varphi_1 L/(2\pi)\}\right] \\ F_b = k_s\left[d_i - \{q_2 - \varphi_2 L/(2\pi)\}\right] \end{cases}. \quad (4)$$

Where k_s, d_i, L, φ_1, and φ_2 are the spring constant, initial length of the spring, the lead of the ball-screw, and rotating angles of the right and left ball-screws, respectively.

C. Differential Kinematic Analysis

In this section, differential kinematic analysis was conducted to obtain the relationship between the force acting on the SEA of the manipulator and the static force applied to the contact part of the compliant manipulator.

First, by differentiating Eq. (1) and (2), the Jacobian can be obtained as follows

$$\begin{bmatrix} \dot{h}_1 \\ \dot{h}_2 \end{bmatrix} = J_{x'} J_x^{-1} J_q \begin{bmatrix} \dot{q}_1 \\ \dot{q}_2 \end{bmatrix} = J \begin{bmatrix} \dot{q}_1 \\ \dot{q}_2 \end{bmatrix}. \quad (5)$$

Where $J_{x'} = \begin{bmatrix} -1 & -(b+c)\cos x_2 \\ -1 & (b+c)\cos x_2 \end{bmatrix}$,

$$J_q = \begin{bmatrix} q_1 - b\cos x_2 & 0 \\ 0 & q_2 - b\cos x_2 \end{bmatrix},$$

$$J_x = \begin{bmatrix} x_1 + b\sin x_2 & q_1 b\sin x_2 + x_1 b\cos x_2 \\ x_1 - b\sin x_2 & q_2 b\sin x_2 - x_1 b\cos x_2 \end{bmatrix}$$

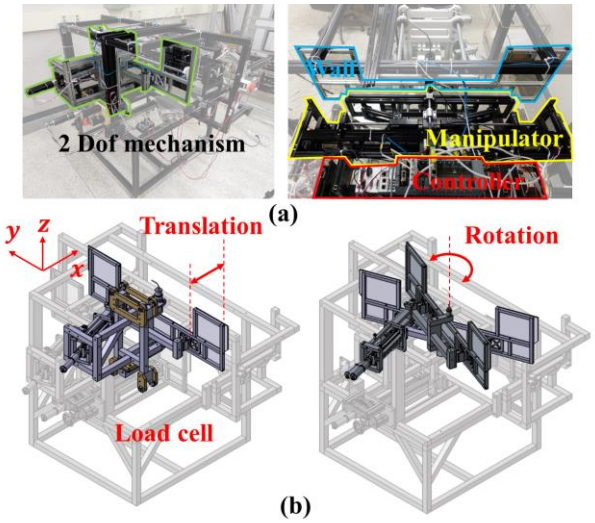

Figure 4. (a) Test bench used for experiments and (b) 2-DOF motions of the wall installed at the test bench and position of load cells

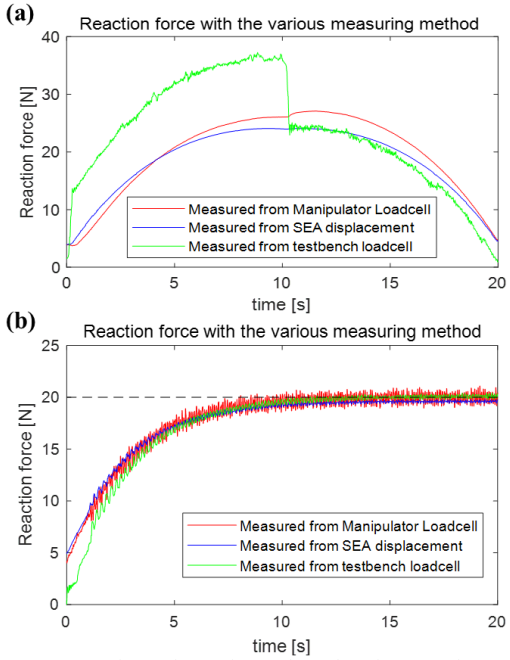

Figure 5. Comparison of experimental results of contact force obtained with various measuring methods when (a) the wall moves or (b) the manipulator moves

Therefore, assuming the static equilibrium state where the manipulator makes contacts with the wall, the force acting on the end of the manipulator can be obtained using the following equation.

$$\begin{bmatrix} F_1 \\ F_2 \end{bmatrix} = \left(J^T\right)^{-1} \begin{bmatrix} F_a \\ F_b \end{bmatrix}. \quad (6)$$

As described above, the posture of the robot is estimated by using the linear encoder and the rotary encoder to obtain the displacement of spring. Thus, using the Jacobian, the contact force of the manipulator contact point can be obtained. In most cases, encoders have a higher resolution and are more robust to signal noise than the load cell, and it is expected that more stable and precise force control will be enabled through the contact force estimated by SEA.

The test bench shown in Fig. 4(a) was designed to verify the reliability of the method of measuring the force at the end of the manipulator. The test bench is equipped with load cells on both sides of the wall to measure the contact force. As shown in Fig. 4(b), the test bench is designed to enable 2-DOF movement with x-axis translation and z-axis rotation.

Because the gondola's carrier is substantial, the distance between the gondola and the wall can be assumed of as moving at a low frequency. From the standpoint of the manipulator, the situation in which the gondola moves can be considered as the situation in which the gondola is stationary, and the walls move. With the fixed posture of the manipulator, the test bench was pushed 20 mm in the x-axis direction at a constant moving speed for 10 seconds, then returned to its original position at the same speed for 10 seconds. The result is shown in Fig. 5(a). It can be seen that an offset exists between the contact force observed in the test bench and the value measured through the displacement of SEA/load cell.

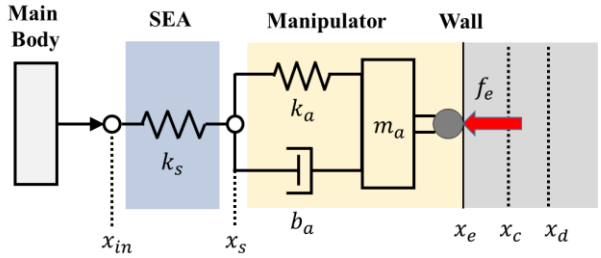

Figure 6. Schematic diagram of the compliant manipulator contacting with environment

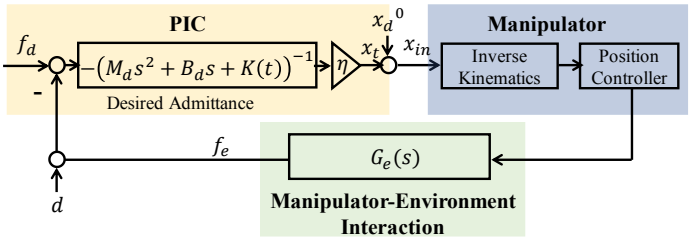

Figure 7. Block diagram of position-based impedance control scheme

It is considered that the component force in the y-axis direction of the contact force acting on the manipulator generates a bending moment in the LM Guide and the linear shaft, which generates the frictional force.

However, it is expected that the influence of friction will be reduced due to the fact that the displacement of the short displacement frequently occurs near the steady-state during feedback control, not when the compression displacement increases or decreases monotonously. Figure 5(b) shows the results of the contact force measurement experiments compared with the position-based impedance controller.

Regarding impedance control, it was confirmed that the estimated value using the load cell/spring could measure the force with an accuracy of ± 5 % based on the measured value of the test bench when the manipulator contacts with the environment.

III. Impedance Control with SEA

A. Position-Based Impedance Control

Impedance control is widely used to control situations involving interaction between the robot manipulator and the environment. Impedance control is used in free space and constrained space with an integrated controller, which realizes compliant motion [11]. However, in certain cases, the impedance controller diverges by the difference between the desired impedance and the actual impedance.

Generally, when the desired mass designed for impedance control in less than the actual mass, the system fails to attenuate disturbances, since the sign of the feedback gain changes [8]. Further, the system becomes unstable when a manipulator with high stiffness is controlled with a low desired stiffness [9]. When using the proposed position-based impedance control, good force tracking performance is achieved by updating the desired stiffness. Therefore, the actual stiffness of the system has a significant effect when applying this controller [6].

In a stiff environment, when the actual impedance is $Z_a(s) = m_a s^2 + b_a s + k_a$ and the stiffness of the wall is k_s, the equation of motion is as follows.

$$\begin{aligned} k_s(x_{in} - x_s) &= k_a(x_s - x_c) + b_a(\dot{x}_s - \dot{x}_c) \\ k_a(x_s - x_c) + b_a(\dot{x}_s - \dot{x}_c) &= k_e x_c + m_a \ddot{x}_c \end{aligned} . \quad (7)$$

In the Laplace domain, Eq. (7) can be written as

$$X_c(s) = \frac{b_0 s + b_1}{a_0 s^3 + a_1 s^2 + a_2 s + a_3} X_{in}(s) . \quad (8)$$

Where $a_0 = m_a b_a$, $a_1 = m_a(k_s + k_a)$, $a_2 = b_a(k_s + k_e)$, $a_3 = k_s k_a + k_s k_e + k_e k_a$, $b_0 = b_a k_s$, and $b_1 = k_a k_s$.

$X_{in}(s)$ and $X_c(s)$ are the Laplace transforms of the motor position input x_{in} and the compliant position of manipulator x_c , respectively.

The force acting on the manipulator can be obtained as follows.

$$F_e(s) = -k_e X_c(s) = G_e(s) X_{in}(s) . \quad (9)$$

By combining Eqs. (8) and (9), transfer function for the coupled system G_e is obtained when there is an interaction between the manipulator and the environment.

The position-based impedance controller applied for the manipulator control with SEA is shown in Fig. 6. At this time, the desired impedance is the same as Eq. (10), and a PD type controller is used in the manner shown in Eq. (11).

$$M_d \ddot{x}_{dc} + B_d \dot{x}_{dc} + K(t) x_{dc} = -E_f (E_f = f_d - f_e) . \quad (10)$$

$$\begin{cases} K(t) = (k_p E_f + k_d \dot{E}_f) x_{dc}^{-1} + k_0 \\ x_{in} = x_d^{\,0} + \eta x_{dc} \end{cases} . \quad (11)$$

By combining Eqs. (10) and (11), the relation between the controller output and the force tracking error can be obtained as follows.

$$X_t(s) = -(\eta + 1) \frac{k_d s + (k_p + 1)}{M_d s^2 + B_d s + k_0} E_f(s) = C(s) E_f(s) . \quad (12)$$

According to the small gain theorem, the above feedback loop is stable when the following conditions are guaranteed.

$$\left\| C(jw) G_e(jw) \right\|_\infty < 1 . \quad (13)$$

The conditions necessary to satisfy the above equation are as follows.

$$\frac{1}{k_s} > (\eta + 1) \frac{k_p + 1}{k_0} - \frac{1}{k_e} - \frac{1}{k_a} . \quad (14)$$

Based on Eq. (14), the following is the stability condition for a given impedance controller when the actual stiffness changes depending on the type of manipulator used in the stiff environment. Controller gain is selected as $\eta = 5$, k_p =5, $k_d = 0.1$, and a stiff environment is assumed.($k_e = 1.0e9$ *N/m*)

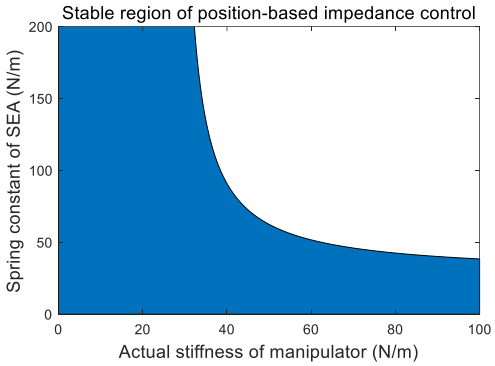

Figure 8. Stable region of spring constant with stiff manipulator

$$\text{Case 1) } (\eta+1)\frac{k_p+1}{k_0} \le \frac{1}{k_e}+\frac{1}{k_a}$$

It is determined that the above inequality holds for all values greater than zero when $k_a \le 27.8\ N/m$. In other words, the impedance controller is stable even without SEA because the stability condition is satisfied for infinitely large k_s. In this case, the smaller the actual stiffness, the smaller the amplitude of the system response. When the impedance controller is applied without SEA, the softer the actual stiffness of the manipulator, the more stable the system.

$$\text{Case 2) } (\eta+1)\frac{k_p+1}{k_0} > \frac{1}{k_e}+\frac{1}{k_a}$$

In Case 2, Fig.8 shows the range of stiffness that the spring can have so that the given impedance controller remains stable when the actual stiffness is changed. As shown in Fig.8, the higher the actual stiffness of the manipulator, the smaller the spring stiffness used in the SEA, and the more stable the given system. Therefore, with knowledge of the actual stiffness range of various modular cleaning modules that can be attached to the cleaning robot, it is possible to guarantee the controller stability regardless of the desired stiffness range by selecting an appropriate spring.

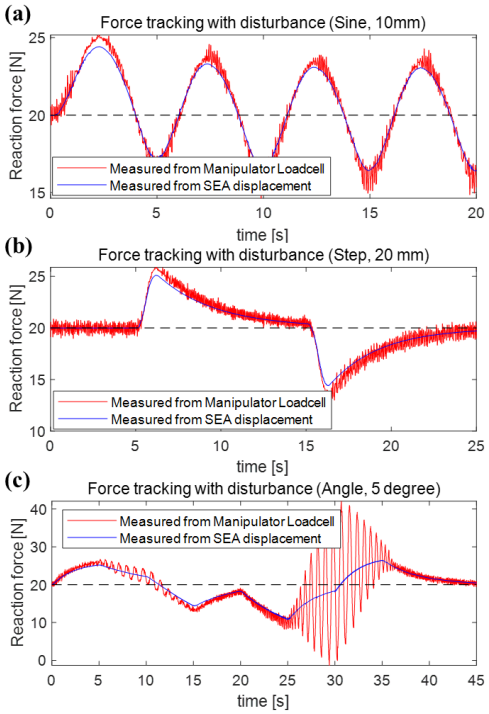

Figure 9. Force tracking performance of proposed manipulator with different measuring methods with disturbances of (a) sinusoidal, (b) step, and (c) angle

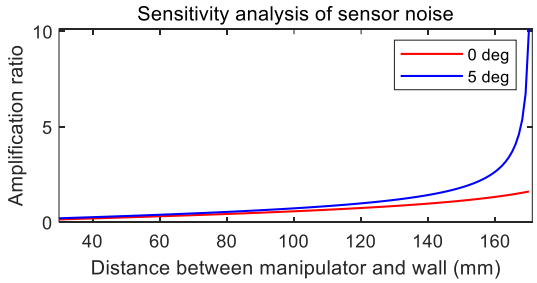

Figure 10. Sensitivity analysis of sensor noise

IV. Experimental Results

The force tracking performance of the proposed compliant mechanism with a position-based impedance controller is experimentally verified. The experiment was conducted using the same test bench shown in Fig. 4. The three most frequent types of disturbance between the wall and the manipulator were considered for experiments.: In the first case, the distance between the outer wall and the end effector changes with a periodic function of 0.2 Hz with an amplitude of 10 mm. In the second case, there are 20 mm raised frames on the outer wall. In the third case, the outer wall has a slope of ± 5 degrees. The desired force was 20 N.

First, the force tracking controller using data calculated from the displacement of spring and the same controller using data from the load-cell sensor, which is connected to the spring, are tested in the three cases described above. The stiffness of the tested spring is 1 N/mm.

Fig.9 shows the effect of sensor noise on the force tracking performance when applying SEA. The sensor noise measured in the load cell is within ± 0.5 N, but since the frequency is more than 10Hz and the bandwidth of the actuator is narrower than the noise, the sensor noise negatively affects the force tracking performance. On the other hand, the force can be measured without a noise with a resolution under 0.02 N when using the displacement of the SEA, because the resolution of the linear encoder used to calculate the manipulator's posture is 20 um and the resolution of the rotary encoder is 1/12000. Therefore, more stable force control is achieved when using SEA displacement data. In addition, as shown in Fig. 9(c), the performance of the controller using load cell data is not stable and even vibrates at the maximum amplitude of 42 N in the 5-degree slope disturbance case. This is attributed to the larger angle and longer distance between the wall and the end effector as well as the greater singularity of the manipulator, as shown in Fig. 10. Although the noise does not change, the noise is amplified near the singularity to increase the control input error and degrade the controller performance due to the characteristics of the parallel robot mechanism.

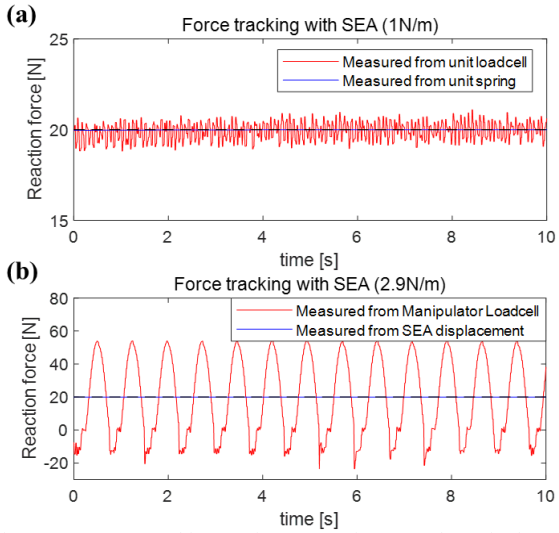

Figure 11. Force tracking performance of proposed manipulator with different stiffnesses of (a) 1N/m, (b) 2.9N/m

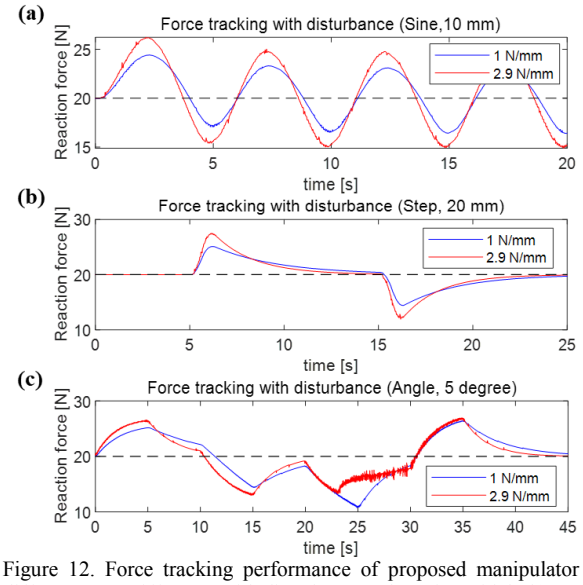

Figure 12. Force tracking performance of proposed manipulator with different SEA stiffnesses with disturbances of (a) sinusoidal, (b) step, and (c) angle

The effect of the spring constant on the stability of the system is shown in Fig. 11. In the case of control by spring displacement, the steady-state error is 0.13 N when using a 1 N/mm spring and 0.46 N when using a 2.9 N/mm spring. When using the load cell data, the Steady-State error is 1.13 N, but when using the 2.9N/mm spring, it emits with an amplitude of 40 N. Therefore, the smaller the spring constant of SEA, the more stable the system was, as confirmed in the previous stability analysis.

The force tracking performance of the impedance controller with the SEA in which the spring constant is either 1 N/mm or 2.9 N/mm is evaluated with changes in the distances and the angles of the upper three cases, and the results are shown in Fig. 12. In this experiment, the results show that the force tracking performance is improved when the spring constant of SEA is low. As shown in Fig. 12(c), vibration occurs at an angle change of 5 degrees. This is attributed to the fact that the configuration of the manipulator approached singularity, which amplifies the error and affects the controller input in the same ways shown in Fig. 9(c).

V. Conclusion

This paper presents the design of a compliant manipulator using a series elastic actuator (SEA) and the mechanism used to precisely measure the force acting on the contact part of the manipulator without a force sensor. It is crucial to maintain constant contact force to ensure good cleaning performance, and the use of a ball screw mechanism can help the system adapt to changes in the distance and the angle between the wall and the manipulator. When the manipulator interacts with the wall of the building, position-based impedance control is used to maintain constant contact force, and the stability of the system has been proven to be secured using SEA regardless of the actual stiffness variation of the manipulator. Here, experiments were conducted in a test bench to demonstrate the force tracking performance of the system against various types of wall changes using a wet-type stiff manipulator. The results indicate that the stiffness of SEA affects the force tracking performance and system stability under the condition of interaction between the manipulator and the environment. In addition, the proposed robust force measurement mechanism for noise improves the stability of the system and improves the control performance.

References

[1] H. Zhang, F. Zhang, W. Wang, R. Liu, G. Zong, "A series of pneumatic glass-wall cleaning robots for high-rise buildings," *Industrial Robot: An International Journal*, vol. 34/2, pp. 150-160, 2007.

[2] T. Akinfiev, M. Armada, S. Nabulsi, "Climbing cleaning robot for vertical surfaces," *Industrial Robot: An International Journal*, vol. 36, pp. 352-357, 2009.

[3] N. Elkmann, D. Kunst, T. Krueger, M. Lucke, T. Felsch, T. Sturze, "SIRIUSc – façade cleaning robot for a high-rise building in Munich, Germany," *Proceedings of the 7th International Conference on Climbing and Walking Robots*, Madrid, Spain, 2004, pp. 1033-1040.

[4] S. Moon, J. Huh, D. Hong, S. Lee, C. Han, "Vertical motion control of building facade maintenance robot with built-in guide rail," *Robotics and Computer-Integrated Manufacturing*, vol. 31, pp. 11-20, 2015.

[5] S. Yoo, I. Joo, J. Hong, C. Park, J. Kim, H. S. Kim, T. Seo, "Unmanned High-Rise Façade Cleaning Robot Implemented on a Gondola: Field Test on 000-Building in Korea," *IEEE Access*, vol.7, pp. 30174-30184, 2019.

[6] T. Kim, H. S. Kim, J. Kim, "Position-based impedance control for force tracking of a wall-cleaning unit," *International Journal of Precision Engineering and Manufacturing*, vol. 17/3, pp. 323-329, 2016.

[7] T. Kim, S. Yoo, H. S. Kim, J. Kim, "Design and Force-Tracking Impedance Control of a 2-DOF Wall-Cleaning Manipulator Using Disturbance Observer and Sliding Mode Control," *2018 IEEE Int. Conf. Robotics and Automation*, pp.4079-4084.

[8] J. J. Wlassich, "Nonlinear force feedback impedance control," M.S. thesis, Dept. Mechanical. Eng., Massachusetts Institute of technology, Massachusetts, United States, 1986.

[9] M. Vukobratovic, D. Surdilovic, Y. Ekalo, D. Katic, *Dynamics and robust control of robot-environment interaction.* Singapore: World Scientific, 2009, ch. 3.

[10] S. Katsura, Y. Matsumoto, K. Ohnishi, "Modeling of Force Sensing and Validation of Disturbance Observer for Force Control," *IEEE Trans. Industrial Electronics*, Vol. 54/1, pp. 530-538, 2007.

[11] N. Hogan, "Impedance control: An approach to manipulation," *American Control Conference*, 1984, pp.303-313.